NUMERICAL SIMULATIONS OF AERODYNAMIC INTERACTIONS BETWEEN MULTIPLE ROTORS

Yasutada Tanabe, Takashi Aoyama and Masahiko Sugiura,
Japan Aerospace Exploration Agency, Tokyo, Japan
Hideaki Sugawara, Ryoyu Systems Co. Ltd., Nagoya, Japan
Shigeru Sunada, Osaka Prefecture University, Osaka, Japan
Koichi Yonezawa, Osaka University, Osaka, Japan
Hiroshi Tokutake, Kanazawa University, Kanazawa, Japan

Abstract

Aerodynamic interactions between multiple rotors on so-called multi-copter UAVs are simulated. The multi-copter UAVs have seen a very rapid and wide spread of applications recently and been mainly used as visual recording platforms. Severe vibrations are often encountered so that gimbal-stabilized camera bases are required. One of the main sources of vibrations is found due to the aerodynamic interactions between the rotors even during hovering flights. A CFD code, rFlow3D, developed in JAXA has been extended to handle multiple rotors. A variable pitch angle controlled hexa-copter is considered with the variation of distance between rotors. The relationship between the oscillatory aerodynamic forces and the rotor distance is investigated. It is found that when the rotor distance is less than half of the rotor radius, the oscillation increases rapidly to nearly 2 times while the rotor performance improves about 10%.

1. INTRODUCITON

Multi-copter UAVs have seen a very rapid and wide spread of applications recently thanks to their simple mechanisms and progress of cheap and reliable MEMS (Micro-Electro-Mechanical Systems) sensors. One of the main applications is the flyable visual recording platform. However, severe vibrations are often encountered on-board so that gimbal-stabilized camera bases are required. One of the main sources of vibrations are considered due to the aerodynamic interactions between the rotors even during hovering flights besides of the mechanical imbalances in the rotating systems.

Most multi-copters adopt propellers with fixed pitch angles. The control of the aircraft is achieved by changing the rotating speed of each rotor. The design of the aircraft became extremely simple where basically no moving mechanical parts such as pitch linkages and swashplates are required. This design is revolutionary compared to the conventional helcopters. However, several disadvantages are also reported. First of all, the multi-copter is considered weak to the turbulent wind. For safe operations, most multi-copters are limited to wind speed of less than 5 m/s. When larger multi-copters with gross weight heavier than 100kg are starting to appear, control through rotating speed seems hard to reach quick response to the gust. Secondly, constant accellerating/de-accellerating of the motor is considered less efficient in power consumption. The loss of control during decent is also often reported for the the multi-copters which may occur as a consequence of the flow stall when the rotating speed is low and the decent speed is high.

The authors are pursuing a design of a hexa-copter with variable pitch angle controls and driven by two large motors placed in the center of the UAV. To demonstrate the advantages of the variable pitch control multi-copter, a prototype as shown in Figure 1 has been manufactured. Because a relatively wider rotor blade is used in this design to ensure plenty control margins in the pitch angles, the interactions between the rotors and the influence of the distance between rotors came to attentions during the design phase. This paper will illustrate the phenomena of the aerodynamic interations between these counter-rotating pairs of rotors through numerical simulations.

Figure 1: A variable pitch control hexa-copter

2. NUMERICAL METHODOLOGIES

Studies of the aerodynamic interactions between

rotors are carried out through numerical simulations using a CFD code, rFlow3D, developed in JAXA for rotorcraft. In the rFlow3D code,[1, 2] a three dimensional moving overlapping grid method is used. This code is originally developed to treat the conventional helicopters where a main rotor and a tail rotor are considered. For the multi-copters, quad (4), hexa (6), octo (8) and even more rotors are used. The data structure in rFlow3D is changed so that a multi-copter with any number of rotors can be handled. Any number of inner background grids can also be placed for efficient capturing of the rotor near wakes.

The full N-S equation in ALE form is shown in Eq. 1, where **U** is the conservative flow variable vector and $\mathbf{F}^i$ and $\mathbf{F}^v$ are inviscid and viscous flux vector respectively. *V(t)* is the time-varying cell volume and *S(t)* is the time-varying cell boundary. **n** is the normal vector to the cell surface.

$$\frac{\partial}{\partial t}\int_{V(t)}\mathbf{U}dV+\oint_{S(t)}\left(\mathbf{F}^i-\mathbf{F}^v\right)\cdot\mathbf{n}dS=0 \tag{1}$$

where,

$$\mathbf{U}=\begin{bmatrix}\rho\\ \rho\mathbf{v}\\ \rho e\end{bmatrix},$$

$$\mathbf{F}^i\cdot\mathbf{n}=\begin{bmatrix}\left(\mathbf{v}-\dot{\mathbf{x}}\right)\cdot\mathbf{n}\rho\\ \left(\mathbf{v}-\dot{\mathbf{x}}\right)\cdot\mathbf{n}\rho\mathbf{v}+p\mathbf{n}\\ \left(\mathbf{v}-\dot{\mathbf{x}}\right)\cdot\mathbf{n}\rho e+p\mathbf{v}\cdot\mathbf{n}\end{bmatrix},$$

$$\mathbf{F}^v\cdot\mathbf{n}=\begin{bmatrix}0\\ \boldsymbol{\tau}\cdot\mathbf{n}\\ \left(\boldsymbol{\tau}\cdot\mathbf{v}-\mathbf{q}\right)\cdot\mathbf{n}\end{bmatrix}$$

The all-speed numerical scheme SLAU (Simple Low-dissipation AUSM) [3] with extension to three dimensional moving grids (referred as mSLAU) is adopted. [4] It is very suitable for the flow calculation around a rotary wing, where the local flow speed may vary from very low on the root area to transonic at the tip. Combining SLAU with a Fourth-order Compact MUSCL TVD (FCMT) interpolation scheme, [5] fourth-order spatial accuracy is obtained in shock free regions. Implicit LU-SGS and Dual-Time-Stepping method [6] are used for time integration on blade grids. Yet for the background grids, explicit four stages Runge-Kutta time integration method [7] is used. In this study, considering the relative low Reynolds numbers on the rotors, no turbulence model is adopted.

The coordinate definitions of the hexa-copter is shown in Figure 2. The rotors are counter-rotating regarding to their neighbours. The aerodynamic forces and moments acting on the center of the hexa-copter can be calculated from Eq. (2).

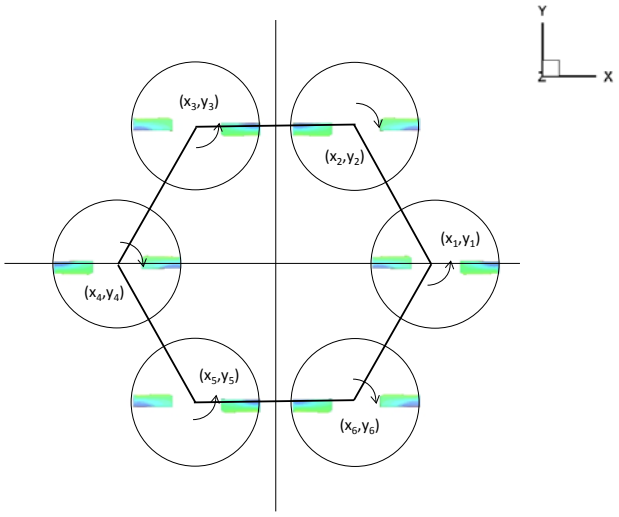

Figure 2: Definition of rotor center coordinates

$$\begin{aligned}
X_{sum}&=\sum_{i=1}^{Nr}X_i\\
Y_{sum}&=\sum_{i=1}^{Nr}Y_i\\
Z_{sum}&=\sum_{i=1}^{Nr}Z_i\\
Mx_{sum}&=\sum_{i=1}^{Nr}Mx_i+\sum_{i=1}^{Nr}Z_iy_i\\
My_{sum}&=\sum_{i=1}^{Nr}My_i+\sum_{i=1}^{Nr}-Z_ix_i\\
Mz_{sum}&=\sum_{i=1}^{Nr}Mz_i+\sum_{i=1}^{Nr}\left\{-X_iy_i+Y_ix_i\right\}
\end{aligned} \tag{2}$$

The rotor forces and moments are non-dimensionalized as in Eq. (3), where the torque and power relationship holds only for a single rotor, remembering that neighbouring rotors are counter-rotating to each other.

$$
\begin{aligned}
C_X &= X/\left(\rho\pi R^2 V_{tip}^2\right) \\
C_Y &= Y/\left(\rho\pi R^2 V_{tip}^2\right) \\
C_Z &= C_T = Z/\left(\rho\pi R^2 V_{tip}^2\right) \\
C_{MX} &= M_X/\left(\rho\pi R^2 V_{tip}^2 R\right) \\
C_{MY} &= M_Y/\left(\rho\pi R^2 V_{tip}^2 R\right) \\
C_{MZ} &= -C_Q = M_Z/\left(\rho\pi R^2 V_{tip}^2 R\right) \\
C_P &= P/\left(\rho\pi R^2 V_{tip}^3\right) = C_Q
\end{aligned}
\tag{3}
$$

3. RESULTS AND DISCUSSIONS

The rotor blade of the prototype of the hexa-copter is shown in Figure 3. The definition of the distance between rotors, d and the distance between the rotor center and the center of the hexa-copter, l is shown in Figure 4. The design parameters for this reference hexa-copter are summarized in Table 1.

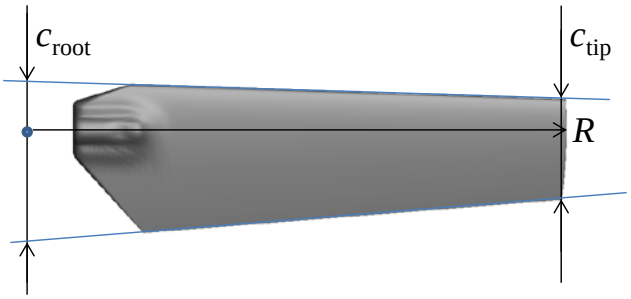

Figure 3: Rotor blade for the prototype hexacopter

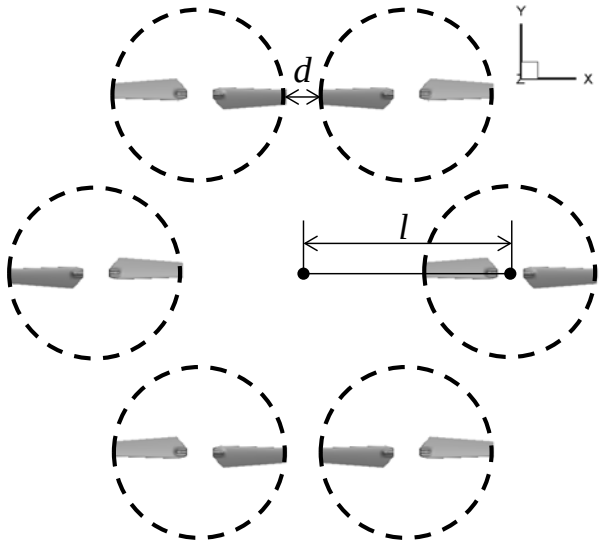

Figure 4: Definition of distances

Table 1: Reference hexacopter design parameters

Hexacopter Original Design Parameters	
Rotor diameter, D	0.330 m
Rotor radius, R	0.165 m
Chord length (c_{root}, c_{tip})	0.0461 m, 0.0290 m
Blade planform	Tapered
Blade twist angle	zero
Blade airfoil	NACA0009
Number of rotors, Nr	6
Number of blades per rotor, Nb	2
Tip Mach number, M_{tip}	0.29412 (100 m/s)
Reynolds number based on chord length	1.99×10^5
Distance between rotor, d	0.063 m (約0.38R)
Distance between rotor center and aircraft center, l	0.393 m

A parametric study is performed by changing the distance between the rotors as shown in Table 2. The pitch angle is fixed to 10 degrees in this study. The layout of the rotors for each rotor distance is shown in Figure 5.

As shown in Figure 6, the outer background grid is common for all the cases. The coverage of the inner background grid is adjusted so that all of the rotating blade grid are contained. The spacing in the inner background grid is common for all the cases where 20% of the mean chord length of the rotor blade is used.

The tip vortex trajectories are shown in Figure 7. For the cases of 0.25 and 0.38 rotor radius, the computations were carried out till 60 rotor revolutions to reach an acceptable quasi-steadiness, while for other longer rotor distance cases, 30 revolutions seem enough. Interactions between the wakes can be clearly observed. When the rotor distance is below 0.5R, the near wakes of the tip vortices are also disturbed.

The time histories of the thrust from the quick starts in the computations are shown in Figure 8. Long period fluctuations are observed in the cases where the rotor distances are below 0.5R. It is considered that the wakes from the hovering multi-rotors are unstable especially when the rotor distance is short. Forces and moments from the final 5 revolutions are used to obtain the level of oscillations.

The six components of forces and moments acting on the center of the hexa-copters are shown in Figure 9 – 13 for each rotor distance respectively. Five revolutions are shown for each case and it is can be observed that with in one revolution, there are two large oscillations and four smaller ones. The

rotors in the computations are rotating in same speed and all starting from a same azimuthal angle. In this hexa-rotor layout, the rotor blade tips of rotor 2 and 3 together with rotor 5 and 6 passing through each other two times at azimuth angle of 0 and 180 degrees which correspond to the two large oscillations. When the blade tips come to near the neighbouring rotor tip path smaller oscillations are observed.

The effects of the rotor distance on the averaged forces and the oscillations are shown in Figure 14. With a fixed pitch angle of 10 degrees, the thrust increases about 4% when the rotor distance is changed from 0.5R to 0.25R. However, the oscillation level of the thrust nearly doubles. The oscillations are measured by the standard deviation and normalized by the averaged thrust. For this case, there are 1-2% oscillatory forces in the total thrust and this may become a strong source of the vertical vibration on board. There are also non-negligible oscillatory pitching and rolling moments as shown in Figure 14 (c). It must be noted that in general multi-copters, the rotating speeds are varying and the relative blade phase angles should be quite random. The oscillatory forces will be more irregular. The influences of the relative phase angle differences on the oscillations for the constant rotating speed multi-rotors will be studied.

Together with the thrust increase, the torque also increases when the rotor distance becomes short. The effect of the rotor distance on the rotor performance is evaluated as shown in Figure 15. Averaged rotor thrust and required torque coefficients for a single rotor is shown in Figure 15 (a) and (b). Figure of merit is shown in Figure 15 (c). It is observed the figure of merit improves about 10% when the rotor distance is 0.25R compared to 0.50R. It is concluded that the design of a multi-rotor should be a compromise between the rotor performance and oscillations.

The spectre of the oscillatory forces and moments are shown in Figure 16. Up to 10/rev components are shown and it is observed that the 2, 4, 6/rev components are dominating here when all the rotor blades are rotating in a same speed and starting from a same phase angle.

4. CONCLUSIONS AND FUTURE WORKS

Aerodynamic interactions between multiple rotors are studied and the influence of the rotor distance is investigated.

The aerodynamic interactions can cause an oscillatory force at a level of 1-2% of the total thrust and have a components in the frequencies of 1-6/revs.

When the rotor distance is less than 0.5R, the oscillation level increases rapidly and is 2 times when rotor distance is 0.25R compared to 0.5R. However, when the rotor distance is larger than 0.5R, the effects of the rotor interactions are nearly the same.

Rotor performance improves when the rotor distance is short. About 10% improvement is observed when the rotor distance is 0.25R. The design of a multi-copter must be a compromise between the rotor performance and the oscillation levels.

Further studies on the interactions between multiple rotors are still ongoing where the phase angle and the pitch angle and the flying speed will be the parameters. The influences of the ceilings and side walls on the rotor performance will also be studied.

ACKNOWLEDGEMENT

This research was funded by ImPACT Program of Council for Science, Technology and Innovation (Cabinet Office, Government of Japan).

COPYRIGHT STATEMENT

REFERENCES

[1] Tanabe, Y., Saito S. and Sugawara, H., Construction and Validation of an Analysis Tool Chain for Rotorcraft Active Noise Reduction, 38th ERF, Amsterdam, NL, Sept. 4-7, 2012.

[2] Tanabe, Y., Saito, S., Takayama, O., Sasaki, D. and Nakahashi, K., A New Hybrid Method of Overlapping Structured Grids Combined with Unstructured Fuselage Grids for Rotorcraft Analysis, 36th European Rotorcraft Forum, Paris, France, September 9-11, 2010.

[3] Shima, E., and Kitamura, K., On New Simple Low-Dissipation Scheme of AUSM-Family for All Speeds," 47th AIAA Aerospace Sciences Meeting, Orlando, FA, January 5-8 2009, AIAA Paper 2009-136.

[4] Tanabe, Y. and Saito, S., “Significance of All-Speed Scheme in Application to Rotorcraft CFD Simulations,” The 3rd International Basic Research Conference on Rotorcraft Technology, Nanjing, China. October, 2009.

[5] Yamamoto, S. & Daiguji, H., “Higher- Order-Accurate Upwind Schemes for Solving the Compressible Euler and Navier-Stokes Equations,” Computers & Fluids, Vol.22, No.2/3, pp.259-270, 1993.

[6] Zhang, L.P. and Wang, Z.J., “A Block LU-SGS Implicit Dual Time-Stepping Algorithm for Hybrid Dynamic Meshes,” Computers & Fluids, Vol.33, pp.891–916, 2004.

[7] Arnone, A., Liou, M.S. and Povinelli, L. A., "Multigrid Time-Accurate Integration of Navier-Stokes Equations," NASA TM-106373, November 1993.

Table 2: Rotor distance parametric study cases

Case No.	Distance between Rotors, *d*	Distance between rotor center and aircraft center, *l*	Note
1	0.25*R*	0.37150 m	
2	0.38*R*	0.39300 m	Reference
3	0.50*R*	0.41250 m	
4	0.75*R*	0.45375 m	
5	1.00*R*	0.49500 m	

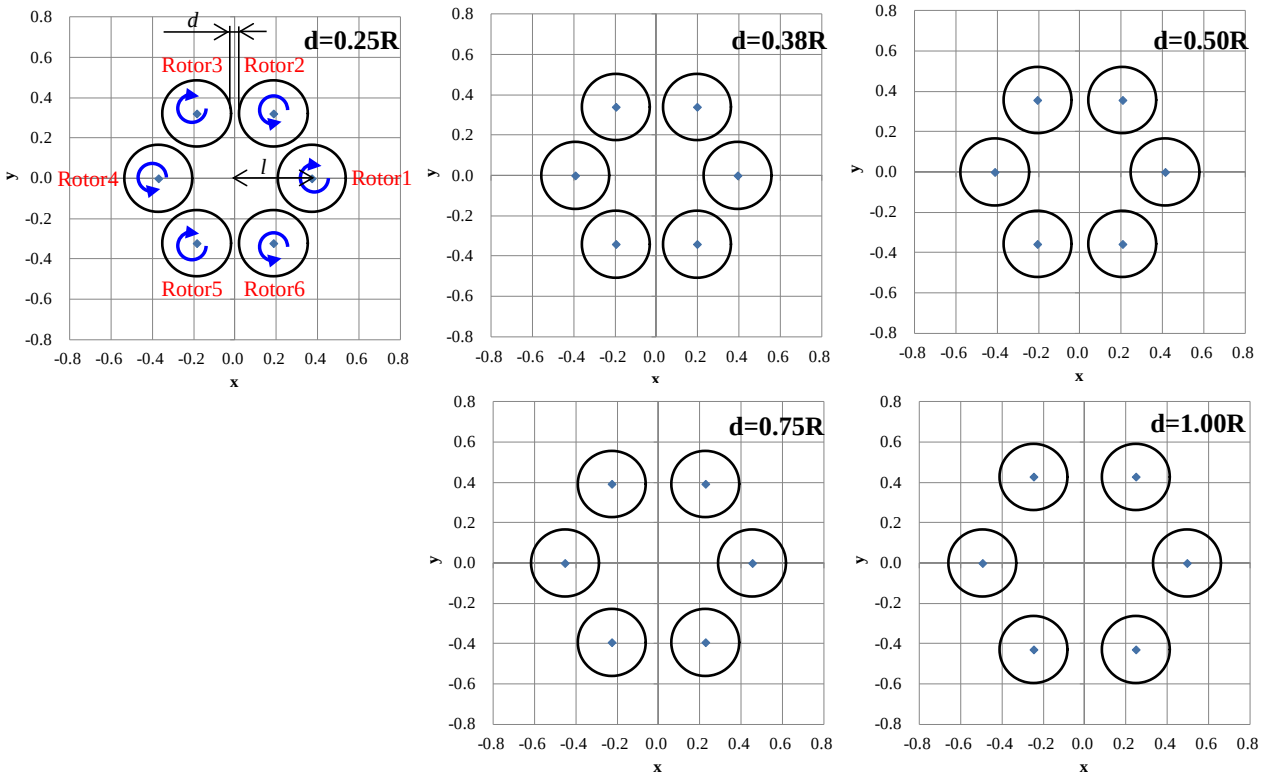

Figure 5: Layout of the rotors for different rotor

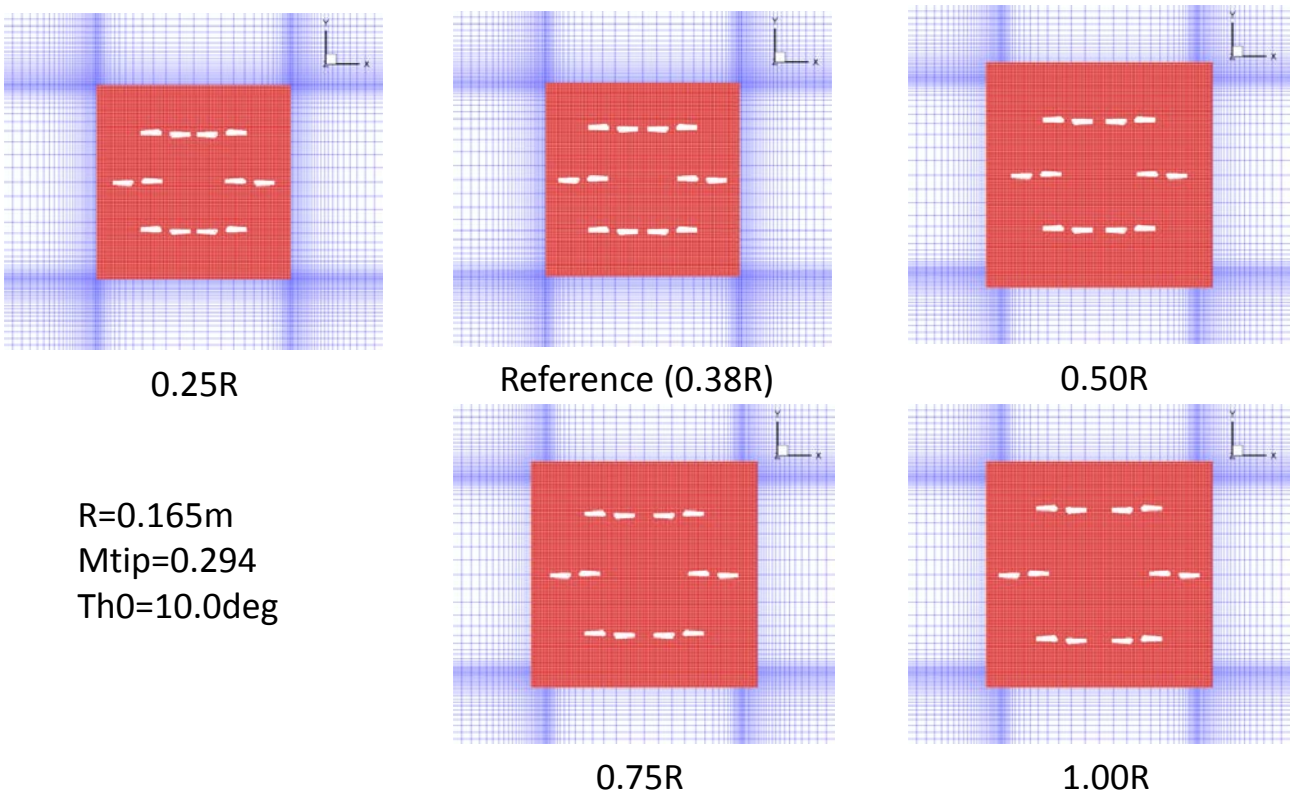

Figure 6: Overlapping grid systems

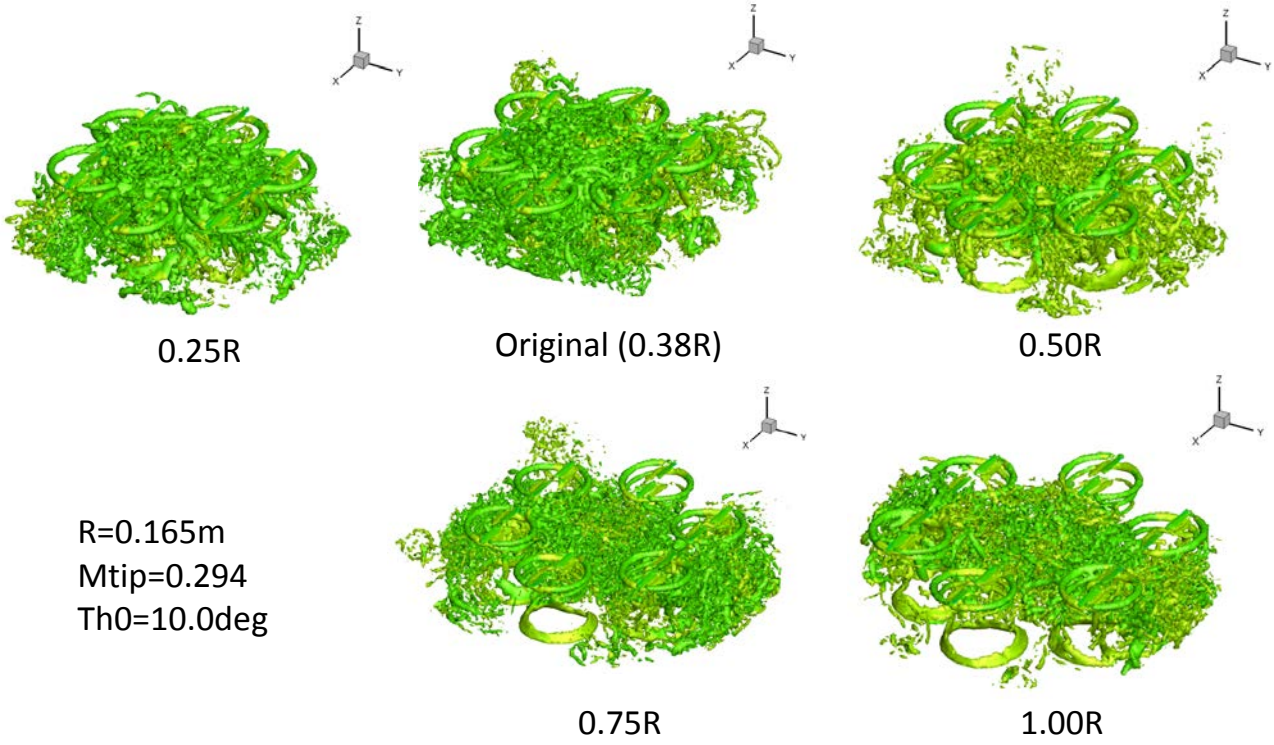

Figure 7: Tip vortex trajectories

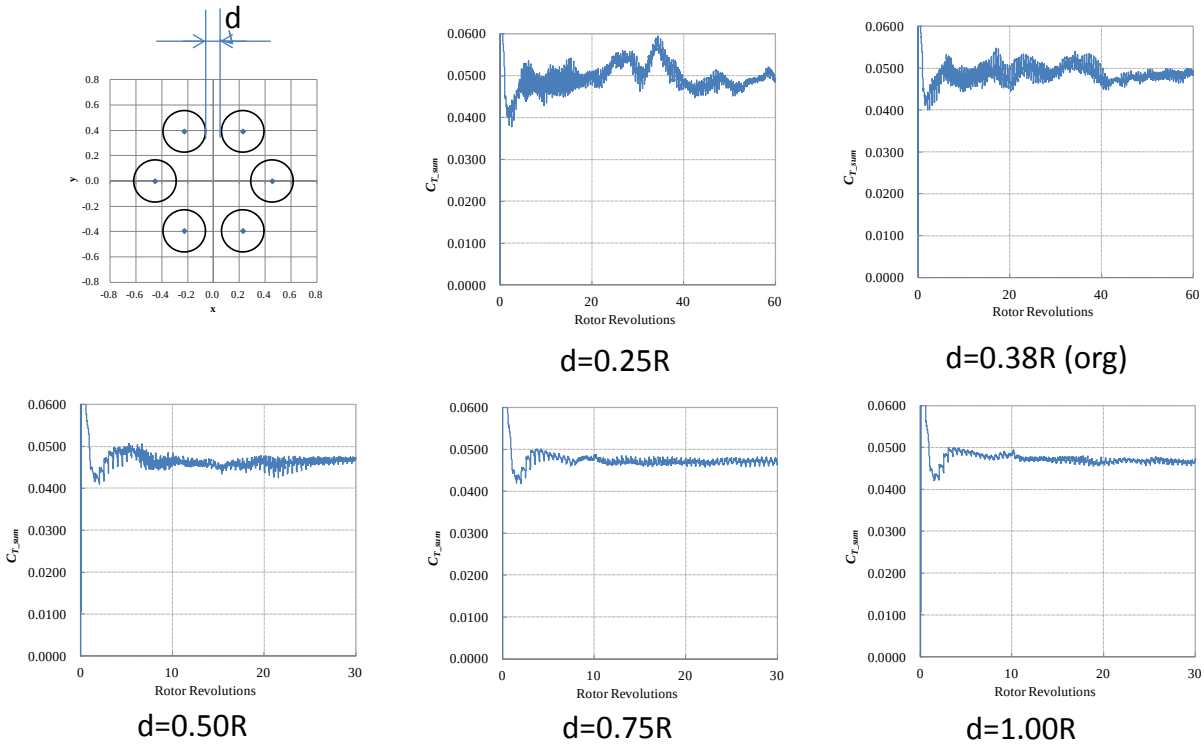

Figure 8: Time histroies of the summed thrust coefficient.

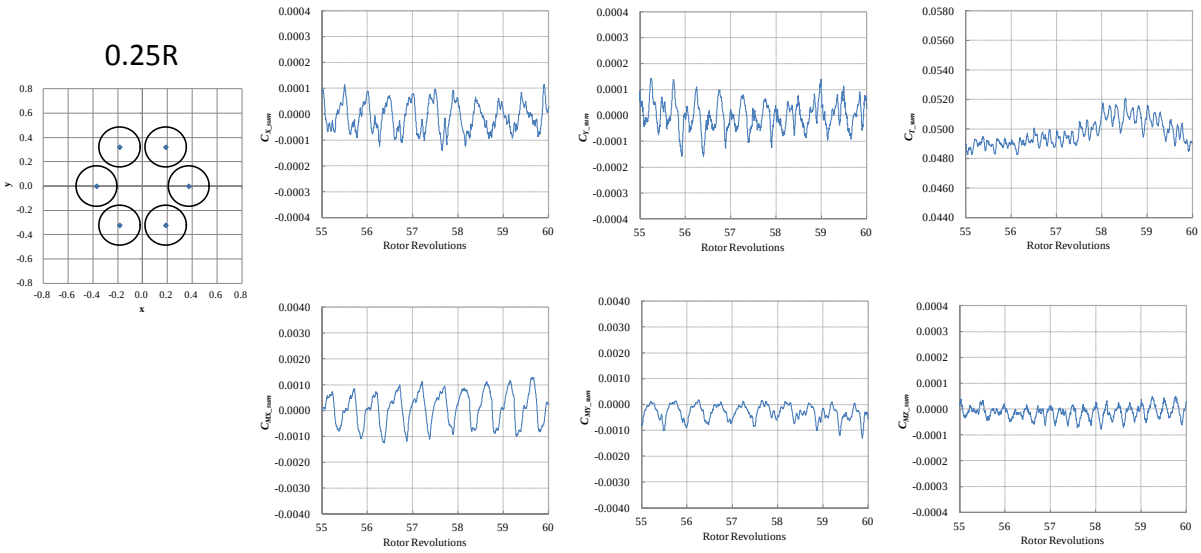

Figure 9: Six components of forces and moments for rotor distance 0.25R

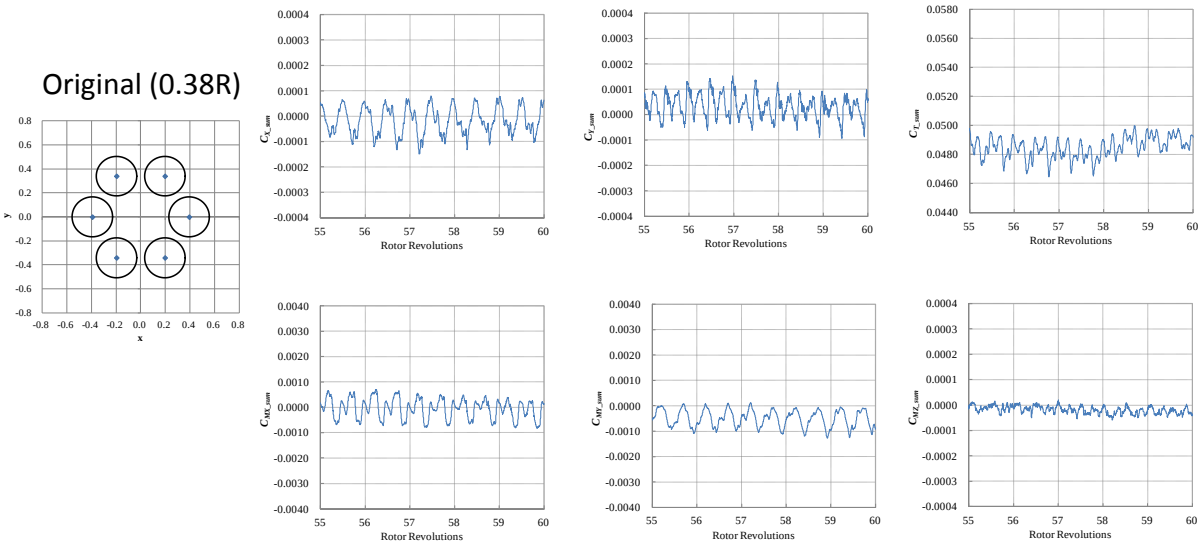

Figure 10: Six components of forces and moments for rotor distance 0.38R (reference design)

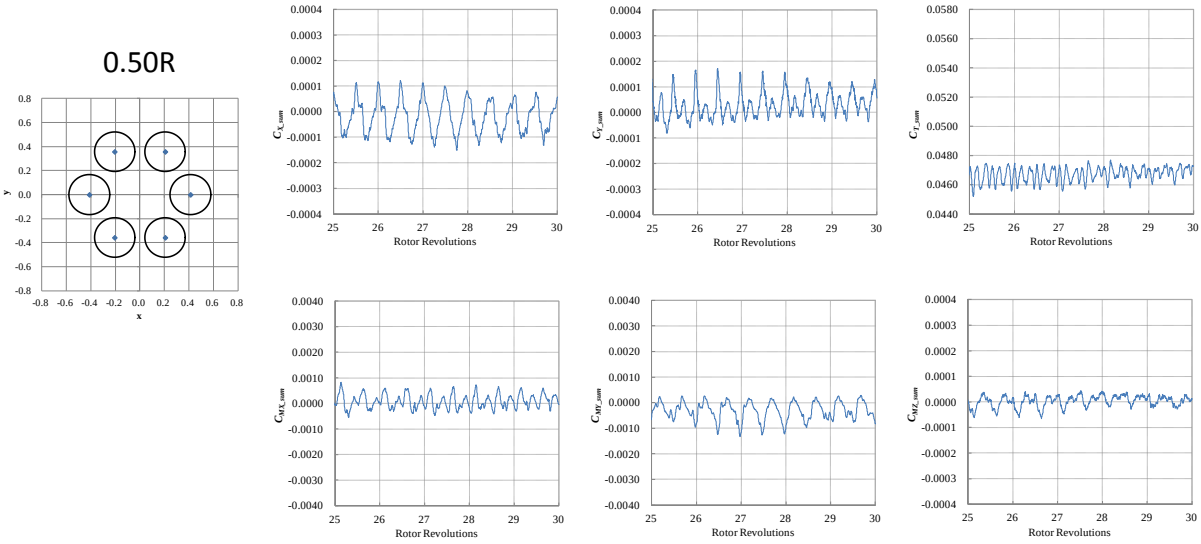

Figure 11: Six components of forces and moments for rotor distance 0.50R

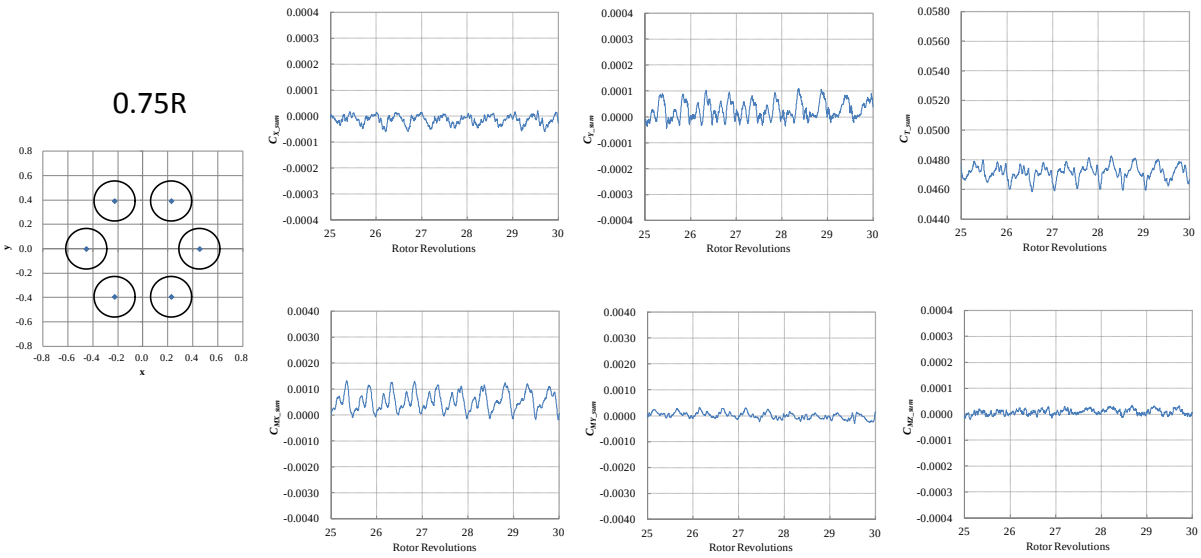

Figure 12: Six components of forces and moments for rotor distance 0.75R

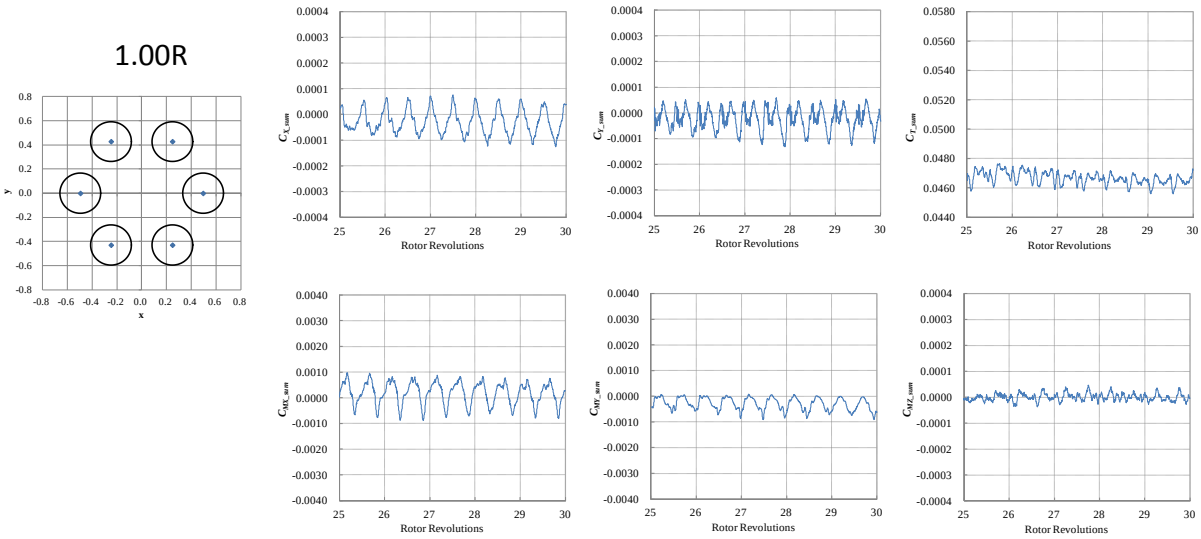

Figure 13: Six components of forces and moments for rotor distance 1.00R

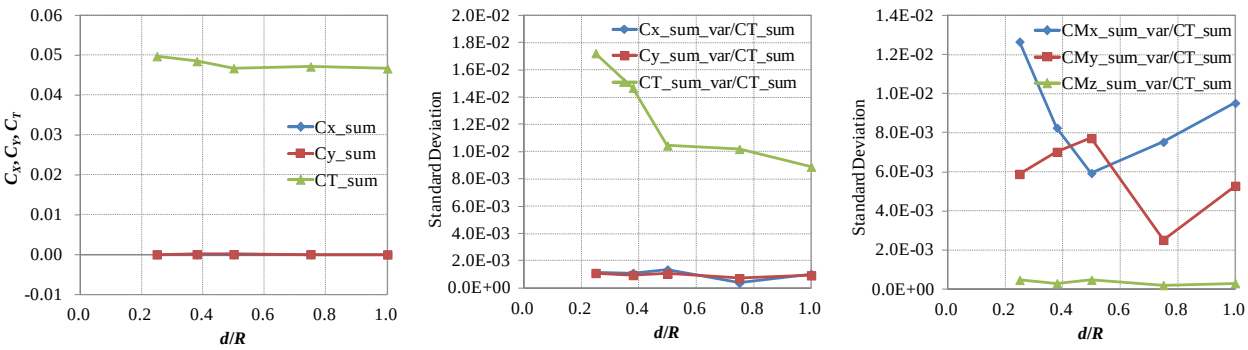

(a) averaged forces (b) variations of forces (c) variations of moments

Figure 14: Effects of rotor distance on averaged forces and variations

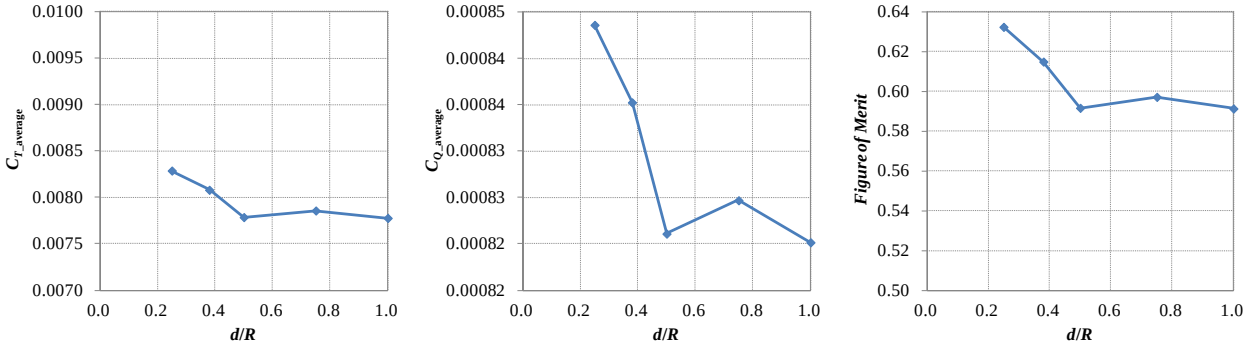

(a) single rotor thrust (b) Single rotor torque (c) single rotor figure of merit

Figure 15: Effect of rotor distance on rotor performance

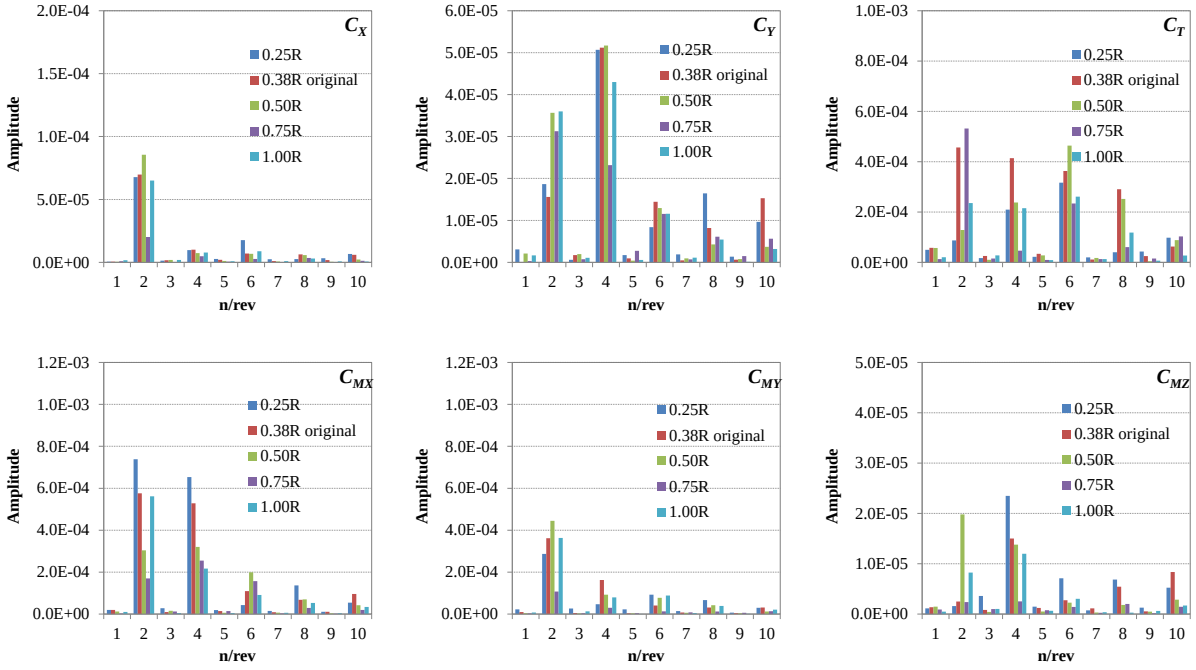

Figure 16: Frequencies of the oscillating forces and moments